1 Introduction and Scientific Motivation

Fast outflows that absorb X-ray and UV radiation are common in AGN. In luminous Broad Absorption Line quasars (BALQs) these are observed to reach velocities up to a few 10^4 km s^{-1}, and they subtend $\approx$ 10–30% of the sky as viewed from the central source. In lower-luminosity Seyfert galaxies, outflows are observed $\gtrsim$50% of the time although they have considerably lower velocities up to $\approx 10^3$ km s^{-1}. Despite their ubiquity, even the basic properties of these outflows remain poorly understood. *How are the observed X-ray and UV absorption related? Why do some outflows cause strong X-ray absorption while others cause much less? Does the amount of X-ray absorption vary substantially over time? How are the X-ray absorption properties related to the other key properties of the AGN?*

X-ray absorption and α_{ox}: In the X-ray band, absorption by outflowing gas often manifests itself by increasing the observed value of α_{ox}, the slope of a nominal power law connecting rest-frame 2500 Å and 2 keV (e.g., Brandt, Laor, & Wills 2000, hereafter BLW); AGN with large α_{ox} are weak in the soft X-ray band relative to their optical emission. In a systematic study of the $z < 0.5$ Palomar-Green (PG) AGN, BLW discovered a very strong correlation between α_{ox} and the EW of blueshifted C IV absorption, supporting the idea that X-ray absorption is the primary cause of large α_{ox} (see Fig. 1a). Selection upon α_{ox} has allowed the construction of well-defined samples of AGN that are likely to suffer from absorption. PG AGN with $\alpha_{ox} > 1.75$ usually show complex X-ray absorption with $N_H \approx 10^{21}$–10^{23} cm^{-2}, as has been directly confirmed by hard X-ray spectroscopy (e.g., Gallagher et al. 2001, 2002). Finally, PG AGN with large α_{ox} have been found to show a strong correlation between maximum UV absorption velocity (v_{max}) and optical luminosity (M_V), suggesting that v_{max} is largely set by the luminosity (Laor & Brandt 2002, hereafter LB). This correlation is predicted by some radiation-pressure driven outflow scenarios, and it promises to provide a unified understanding of the outflows seen in Seyfert galaxies and quasars.

A systematic PG X-ray absorption survey: One of the main limitations in extending our understanding of obscuring AGN outflows has been the lack of systematic X-ray spectroscopy for a well-defined sample of significant size, particularly since the X-ray absorbing gas might well comprise most of the mass in the outflow. Current X-ray spectroscopy has been confined to the study of just a few objects, making it difficult to draw broad conclusions. Here we propose to remedy this situation with *XMM-Newton* by completing the X-ray spectroscopic coverage of all 13 $z < 0.5$ PG AGN with $\alpha_{ox} > 1.75$. We will determine the X-ray absorption and underlying continuum properties of this well-defined sample, and we will search for connections between the X-ray absorption properties and other key AGN properties.

2 Target Selection, Proposed Observations, and Science Goals

We have selected our targets from the PG AGN sample, due to the excellent multiwavelength coverage already in hand for these bright AGN (see Table 1). We have selected targets that (1) have $\alpha_{ox} > 1.75$, (2) should be X-ray bright enough for good EPIC spectroscopic constraints, and (3) do not already have sufficient X-ray spectra. Observations of all of these targets will complete the X-ray spectroscopic coverage of the most heavily absorbed AGN in the PG sample, allowing general conclusions to be reached (see above and Fig. 1a).

Exposures and priority: Our proposed exposure times of 23–43 ks (including overhead) are the most economical that will provide effective EPIC spectroscopy. We have calculated these times based on the currently available X-ray data; all of our targets have X-ray detections that allow reasonable estimates of *XMM-Newton* spectral quality. We have prioritized our targets based upon their multiwavelength absorption properties as well as their expected X-ray fluxes.

As discussed below, only two of our targets (PG 1011–040 and PG 2251+113) have broad-band X-ray spectroscopic coverage with *ASCA* or *BeppoSAX*. In both cases the current X-ray data are insufficient for reliable X-ray absorption studies; the improved throughput of *XMM-Newton* will enable such studies for the first time. Many of our targets have notable UV absorption (e.g., see

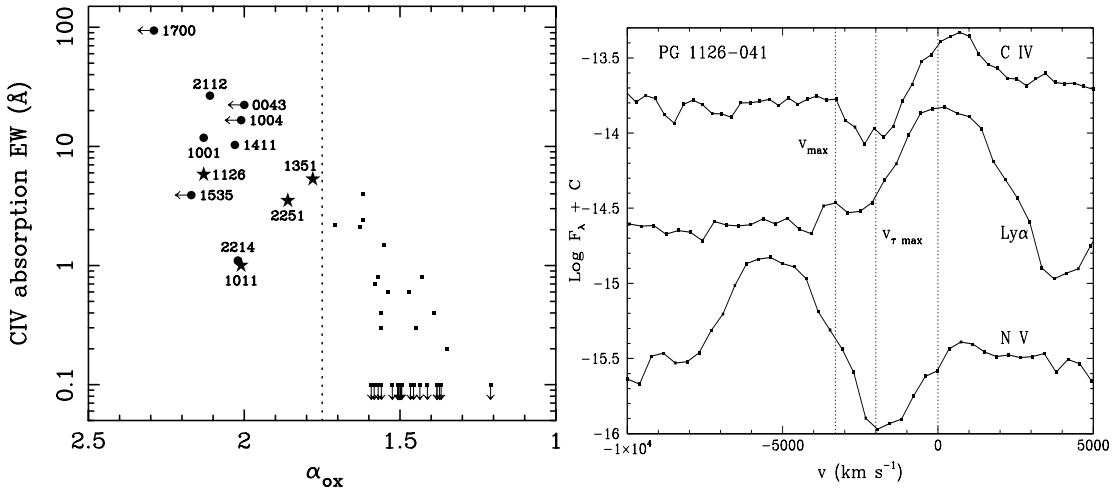

Figure 1: **(a)** The C IV absorption EW vs. α_{ox} relation for the $z < 0.5$ PG AGN (adapted from BLW and LB). The objects with $\alpha_{ox} > 1.75$ are designated by the right ascension parts of their names. Stars are the targets proposed here, and large filled circles are objects with sufficient X-ray coverage already. Small filled squares are objects with weak or no X-ray and UV absorption. **(b)** UV absorption lines seen in *IUE* velocity spectra of PG 1126–041 (adapted from LB).

Fig. 1b), polarization, and other properties as described in the object notes below.

Science goals: Our main science goals are to characterize the X-ray absorption and continuum properties of these PG AGN. We expect to detect significant X-ray absorption in our objects, and we will fit our data with the best available ionized-absorber and partial-covering models to determine the nature of the absorption. The key absorption parameters to be measured include the column density, ionization parameter, and covering fraction. We will also search for long-term variability of the absorption by comparison with archival X-ray data. At high energies (above $\approx$ 2–5 keV) where the effects of absorption are minimized, we should be able to obtain clean measurements of the underlying power-law continuum strength and shape (provided the absorbing column density is $\lesssim 10^{24}$ cm^{-2}). With these, we will be able to determine if these AGN have typical underlying continua (both in terms of α_{ox} and photon index). For calculating α_{ox} we will obtain simultaneous OM measurements of the optical and UV fluxes.

In some cases we should obtain enough photons to study iron Kα spectral features and rapid X-ray variability. For example, we will search for strong, blueshifted iron Kα absorption lines and edges from highly ionized gas in the quasar outflows (see Chartas et al. 2002 and Pounds et al. 2003). We will also fit any detected iron Kα emission lines to constrain X-ray reflection in the nuclear environment. Detection of rapid X-ray variability would show that we are observing the underlying X-ray continuum source directly (rather than via a large-scale scattering "mirror" of electrons). Finally, while we expect the RGS data to have low signal-to-noise given the proposed observation lengths, we will search for any strong spectral features in these data.

With complete X-ray coverage of the PG AGN with $\alpha_{ox} > 1.75$ (using both these data and archival data), we will search for connections between the X-ray absorption properties, the X-ray continuum properties, and other key AGN properties. This is the ideal sample for such work due to the enormous database of high-quality and uniform data available for the PG AGN. The $\alpha_{ox} < 1.75$ PG AGN will serve as an excellent control sample so that reliable statistical inferences can be drawn, and we will also make comparisons with soft X-ray weak quasars found in grism (e.g., Risaliti et al. 2003) and near-infrared (e.g., Wilkes et al. 2002) surveys. For example, we will investigate if the X-ray absorption properties correlate with the strength, width, minimum velocity, or maximum velocity of the observed UV absorption. Detection of such correlations is the logical way to extend the relation shown in Fig. 1a, and such correlations will give insight into the structure and dynamics of the outflow. Our $\alpha_{ox} > 1.75$ sample spans a range of C IV

Target Name	z	$B/M_{\rm V}$	$\alpha_{\rm ox}$	Exp. (ks)	Cts.[1]	Notes and References to X-ray Spectral Models
PG 1351+640	0.087	15.4/−23.3	1.78	23	20,500	Mini-BALQ; Zheng et al. (2001)
PG 1126–041	0.060	15.4/−22.3	2.13	33	9500	Mini-BALQ; BLW; Wang et al. (1999)
PG 1011–040	0.058	15.5/−22.0	2.01	43	5200	UV absn?; LB; Gallagher et al. (2001)
PG 1552+085	0.119	16.0/−23.0	1.77	23	18,500	BALQ?; Turnshek et al. (1997)
PG 2251+113	0.323	16.3/−25.4	1.86	33	8900	Mini-BALQ; BLW; LB

Table 1: PG 1351+640 is the highest priority target and PG 2251+113 the lowest. PG 2251+113 is a steep-spectrum radio-loud quasar; all other targets are radio-quiet. Luminosities are computed adopting $H_0 = 70$ km s^{-1} Mpc^{-1}. [1]This column shows the estimated number of EPIC pn+MOS counts (see §3).

absorption EW of 1–94 Å and a range of maximum UV absorption velocity of 2000–31,000 km s^{-1}; we will be able to study systematically the UV/X-ray absorption connection from the associated UV absorber level, through mini-BALQs, to the BALQ absorber level. Furthermore, in cases where partial covering X-ray absorption is detected, a relation between the partial covering fraction and polarization is likely; partial covering often arises due to electron scattering of X-rays, and such scattering can also polarize optical and UV light. LB have shown that luminosity effects are important in setting many of the UV absorption properties (see §1), and we will extend this work by searching for correlations between luminosity and X-ray absorption properties. Finally, we will search for X-ray absorption correlations with the optical emission-line properties. Of particular interest will be those line properties associated with "eigenvector 1" of Boroson & Green (1992), since these appear related to $L/L_{\rm Edd}$. Black hole masses have also been estimated from the optical emission-line properties (e.g., Laor 1998) and will be used in the correlation analyses.

Target notes: ***PG 1351+640*** has strong, complex UV absorption extending to ≈ 3000 km s^{-1}, making it a mini-BALQ (e.g., Zheng et al. 2001 and references therein). Note that we have also proposed PG 1351+640 for a much longer *XMM-Newton* observation in a separate proposal (designed to obtain RGS spectral constraints). If this much longer observation is accepted then we withdraw the shorter observation of PG 1351+640 proposed here. ***PG 1126–041 (Mrk 1298)***, a mini-BALQ, has UV and X-ray absorption which have been studied by Wang et al. (1999) and LB (see Fig. 1b). However, the *ROSAT* data are of limited quality (≈ 320 counts), and the X-ray absorption properties are not well constrained. ***PG 1011–040*** appears to have UV absorption based on the available *IUE* data (LB). Our 35 ks *ASCA* observation of this source did not reveal any obvious X-ray absorption, presenting the intriguing possibility that this could be an intrinsically X-ray weak AGN. However, the *ASCA* photon statistics were limited, and a better X-ray spectrum is clearly needed (Gallagher et al. 2001). ***PG 1552+085*** appears to have UV absorption in *IUE* data and has been claimed to be a BALQ (Turnshek et al. 1997). However, from the noisy *IUE* data the C IV EW cannot be reliably measured (BLW); it therefore does not appear in Fig. 1a. PG 1552+085 has relatively high optical continuum polarization, P=1.9% (Berriman et al. 1990). ***PG 2251+113*** is a radio-loud mini-BALQ (e.g., BLW, LB), and a high-quality UV spectrum of it will be obtained during *HST* Cycle 12. The current *ASCA* data are unable to distinguish between an absorbed X-ray spectrum and an intrinsically flat X-ray spectrum, although the former seems more likely (BLW). Better statistics from *XMM-Newton* are clearly required.

Need for XMM-Newton: The large effective area of *XMM-Newton* is required to perform CCD X-ray spectroscopy of these objects in an economical manner. We require 4000–20,000 source photons to achieve our science goals. *Chandra* and other currently operating X-ray satellites simply cannot collect enough photons with reasonable observation lengths. Furthermore, the broad bandpass of *XMM-Newton* EPIC makes it ideal. The 2–10 keV sensitivity is required to constrain the underlying continuum as well as iron Kα spectral features, and the soft 0.3–2 keV response will enable detailed absorption studies.

Supporting data: Aside from the data mentioned above, we will obtain near-simultaneous optical spectroscopy with the 8-m Hobby-Eberly Telescope (30% owned by Penn State). We will

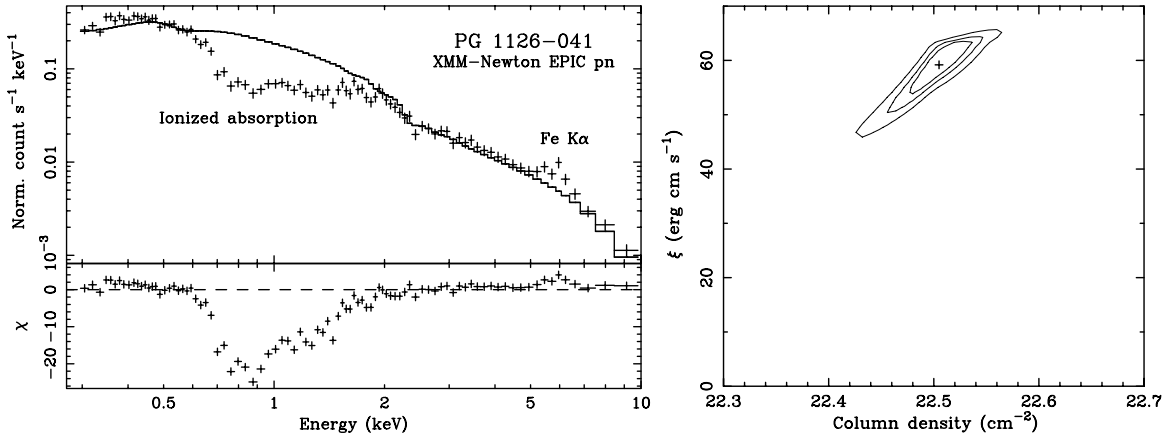

Figure 2: **(a)** Simulated 30 ks EPIC pn spectrum of PG 1126–041 based on fitting of the *ROSAT* data with an ionized absorber model. The underlying power-law continuum has $\Gamma = 2$ and a 2–10 keV flux of 4.9×10^{-13} erg cm^{-2} s^{-1}. The ionized absorber has $N_{\rm H} = 3.2 \times 10^{22}$ cm^{-2} and $\xi = 60$ erg cm s^{-1}, and a narrow iron Kα line with an EW of 150 eV has been included. To make the plot, the continuum above 2.5 keV has been fit with a power-law model which has then been extrapolated to lower energies. Note the clear systematic residuals due to the absorption and the iron Kα line. **(b)** Confidence contours (68, 95, and 99%) derived when fitting the PG 1126–041 pn and MOS spectra with an ionized absorber model.

also propose supporting *HST* UV spectroscopy to allow a simultaneous or near-simultaneous study of X-ray and UV absorption.

3 Additional Technical Feasibility Issues

Expected counts: Our targets are optically bright PG AGN, and all of them have X-ray detections. These X-ray data, combined with the best available X-ray spectral models in the literature, have been used to calculate the expected number of EPIC pn+MOS counts. We have used SCISIM and XSPEC in our count calculations and have been fairly conservative with them. Table 1 gives the expected counts and references to the X-ray spectral models. The pn typically provides $\approx 60\%$ of the counts, and the MOS provides $\approx 40\%$. Due to long-term X-ray variability and uncertainty in the spectral models, the number of counts could be higher or lower by $\sim 50\%$.

Spectral quality: In Fig. 2a, we show one of our simulated spectra for PG 1126–041. To generate this, we have used the archival *ROSAT* data to constrain a power-law model with ionized absorption. With *XMM-Newton*, we can clearly discriminate between partial covering and ionized absorption ($> 99.9\%$ confidence), and we can constrain the absorber parameters as shown in Fig. 2b. We can also detect an iron Kα line with an EW of 150 eV with $> 98\%$ confidence (using the F-test), and we should be able to detect any X-ray variability by $\gtrsim 15\%$ during the observation. Our targets have low Galactic column densities of $(2.5\text{–}5.5)\times 10^{20}$ cm^{-2}; these have been taken into account in all calculations above and will not cause significant difficulty.

Other issues: All of our targets are visible for the proposed exposures. None of our targets will suffer significant contamination from nearby sources. Our OM modes satisfy the brightness and dose constraints.

Berriman G., et al., 1990, ApJS, 74, 869
Boroson T.A., Green R.F., 1992, ApJS, 80, 109
Brandt W.N., Laor A., Wills B.J., 2000, ApJ, 528, 637 (BLW)
Chartas G., et al., 2002, ApJ, 579, 169
Gallagher S.C., et al., 2001, ApJ, 546, 795
Gallagher S.C., et al., 2002, ApJ, 567, 37
Laor A., 1998, ApJ, 505, L83
Laor A., Brandt W.N., 2002, ApJ, 569, 641 (LB)
Pounds K.A., et al., 2003, MNRAS, in press (astro-ph/0303603)
Risaliti G., et al., 2003, ApJ, 587, L9
Turnshek D.A., et al., 1997, ApJ, 476, 40
Wang T.G., et al., 1999, MNRAS, 307, 821
Wilkes B.J., et al., 2002, ApJ, 564, L65
Wills B.J., Brandt W.N., Laor A., 1999, ApJ, 520, L91
Zheng W., et al., 2001, ApJ, 562, 152